Journal of Polymers and the Environment (2026) 34:101
https://doi.org/10.1007/s10924-025-03724-z

ORIGINAL PAPER

Functionalizing Calendered PLA/PBAT Films with Natural Food Additives

Ignacio Mena-Prado[1,2] · Marta Fernández-García[1] · Enrique Blázquez-Blázquez[1] · Sara Limbo[3] · Manuela Rollini[3] · Daniele Maria Martins[3] · Juan P. Fernández-Blázquez[4] · Adolfo del Campo[5] · Alexandra Muñoz-Bonilla[1]

Received: 12 September 2025 / Accepted: 8 December 2025

Abstract
Herein, biodegradable and functional films based on PLA/PBAT (Ecovio®) blends were prepared by calandering processing that allows high-quality films and proper blend mixing. To provide functional properties such as antioxidant and antimicrobial activity, food additives were incorporated including sodium stearoyl lactylate (designated as E481) at 5 wt% and bioplasticizers derived from vegetable oils, namely CITREM (E472C) and ACETEM (E472A) at 10 wt%. Chitin nanocrystals were also added to enhance barrier and mechanical properties. The films of around 200 µm thick were produced resulting in uniform and high-quality materials. Scanning electron microscopy and confocal Raman microscopy demonstrated good mixing of PLA and PBAT biopolymers, as well as a homogeneous dispersion of the additives. This effective blending provides excellent mechanical performance, particularly elongation at break, with values approaching 500% for most of the prepared films. The additives had minimal effect on the crystallinity, thermal and barrier properties while imparting antioxidant and antimicrobial properties with negligible migration into food simulant media, bellow 0.08 mg/Kg in all the cases. Citroglycerides, mono-and diglycerides of fatty acids and sodium stearoyl lactylate provides Trolox equivalent antioxidant capacity (TEAC) values between 14 and 18 µmol Trolox/g, and were effective against Gram-positive *Staphylococcus aureus* and *Listeria innocua* achieving complete bacterial inhibition at the contact tested concentration (ΔLog CFU/mL: 4.54 and 3.71, respectively). Finally, the disintegration of the films under industrial composting condition was demonstrated; this issue is essential to evaluate the environmental impact of the packaging at the end of its life cycle.

keywords Biodegradable · Functional films · Bioplasticizers · Antimicrobial · Antioxidant

Introduction

General consumers along with legislation aimed at reducing plastic waste, have shifted their focus and financial support toward the development of new systems designed to address problems associated with the slow degradation of plastics, which is a significant environmental concern particularly due to their accumulation in both marine and terrestrial environments. Moreover, the production of plastics is highly controversial due to either the unsustainability of the process and the limited availability of fossil fuels [1].

New opportunities have been opened for the development of bioplastics, which can replace non-biodegradable and fossil-based plastics, in particular in the packaging sector, which is the largest consumer of plastics globally. Bioplastic production is expected to rise driven by new and upcoming mandatories that are either being implemented

✉ Alexandra Muñoz-Bonilla
sbonilla@ictp.csic.es

Adolfo del Campo
adelcampo@icv.csic.es

1 Instituto de Ciencia y Tecnología de Polímeros, ICTP-CSIC, C/Juan de la Cierva 3, Madrid 28006, Spain

2 Facultad de Químicas, Departamento de Química-Física, Universidad Complutense de Madrid, Madrid, Spain

3 DeFENS, Department of Food, Environmental and Nutritional Science, Università degli Studi di Milano, Via G. Celoria 2, Milan 20133, Italy

4 IMDEA Materials Institute, C/Eric Kandel, 2, Getafe, Madrid 28906, Spain

5 Institute of Cerámica y Vidrio, ICV-CSIC, C/Kelsen 5, Campus de Cantoblanco, Madrid 28049, Spain

Published online: 17 April 2026

or waiting to approval. These includes mandatories such as the European Packaging and Packaging Waste Regulation (PPWR, Reg. EU 2025/49) [2], which emphasizes the role of biobased plastics in achieving circular economy and climate goals. However, a key limitation of biopolymers is their generally lower mechanical performance compared to conventional plastics [3–5].

Poly(lactic acid) (PLA), is one of the most used and highly promising biopolymer, synthesized from agro-industrial wastes, among others sources. It is noted for its mechanical strength, which is comparable to that of PE, along with its excellent barrier properties against flavours and aromas and good processability [6]. As a result, PLA has already been employed in food packaging and food contact applications [7]. Further, to enhance the inherent properties, PLA is often reinforced with other polymers or substances. Among the various composites, a promising biodegradable copolyester suitable for packaging is poly(butylene adipate-*co*-terephthalate) (PBAT) which combined with PLA enhances the flexibility and brittleness of PLA while maintaining the disintegration in industrial composting conditions [4, 8]. Additionally, to improve the mechanical properties of PLA and its blends, bioplasticizers are widely incorporated to the formulation [9]. Examples include natural macromolecules such as citric acid esters of mono- and diglycerides, also known as citroglycerides or CITREM (designated as E472C) and acetic acid esters of mono-and diglycerides of fatty acids, also known as ACETEM (designated as E472A). Both are commonly used as emulsifiers in food products and approved by the US FDA (Food and Drugs Administration) [10]. When added to the polymeric materials, these bioplasticizers not only improve mechanical properties but also impart additional functionalities such as antimicrobial and antioxidant properties [11, 12].

Both compounds, CITREM and ACETEM, have demonstrated the ability to plasticize PLA through compression moulding. However, their effects on improving the mechanical properties of PLA/PBAT blends were not significant. This outcome can be attributed to phase separation of both polymers occurring during compression moulding [12]. Indeed, the processing and film formation techniques of such biopolymers also influence their performance [13]. Among the different techniques to obtain thin films, typically, blown filming and calendered rolls are widely employed to achieve high uniformity and smoothness of the film [14, 15]. Also, PLA/PBAT blends with different polymer ratios have been studied using calendered rolls and blown film techniques to produce thin films suitable for food packaging applications. As a result, PLA/PBAT composites have shown a highly homogeneous microstructure when processed via calendering compared to films obtained through extrusion and compression moulding [13].

In particular, calendering is a manufacturing technique used to obtain a thin layer by feeding a polymer throw a sequence of rolls rotating at controlled speeds, allowing precise control of sheet dimensions. Calendered films can be employed to package food products when uniformity, thickness control, high transparency, or improved mechanical properties are required [16].

In this study, a commercial blend of PLA/PBAT, named Ecovio® (containing a 45/55 ratio), was processed by extrusion followed by calender rolling while reinforcing with ACETEM and CITREM plasticizers. To further enhance the properties of the PLA/PBAT blends, sodium stearoyl lactylate (designated as E481) (SL) and chitin particles (CP) were added. Particularly, chitin nanoparticles have been incorporated as a reinforcement to enhance the impermeability of the materials [17, 18]. The addition of particles generally increases mechanical resistances by reinforcing the polymer matrix, resulting in an increase of stiffness while reducing the elongation at break [19]. Additionally, SL is commonly used in food applications to preserve quality and extend shelf life [20]. Acting as a humectant, SL helps to retain moisture in foods and is approved by the FDA as a food additive [14]. In this study, SL was incorporated to increase liquid absorption, with the idea of using these composites in applications such as absorbent pads and in the packaging of bakery products, fruits, or salads. The resulting films were evaluated by comparing properties of the films containing different CITREM and ACETEM and either SL or chitin CP. Properties such as antimicrobial, antioxidant, microstructural, permeability, migration of substances as well as thermal and mechanical properties were analysed and discussed.

Materials and Methods

Materials

Ecovio® pellets (Fblend C2224 density: 1.24–1.26 g/cm^3; melt flow index: 2.5 g/10 min) purchased from the Company BASF (Ludwigshafen, Germany).

Different compounds were employed as bioplasticizers for Ecovio® samples, as follows:

GRINDSTED® ACETEM SOFT-NSAFE (CAS number 736150–63 − 3), an acetic acid ester of monoglycerides (E 472a) made from fully hydrogenated castor oil, was obtained from Danisco.

GRINDSTED® CITREM LR 10 EXTRA KOSHER (CAS number 97593–31 − 2) (Product code 173636), a citric acid ester of mono-diglyceride (E 472c) made from edible, refined sunflower oil, was obtained from Danisco. This

product also contains alpha-tocopherol (E 307) max. 200 ppm and ascorbyl palmitate (E 304) max. 200 ppm.

GRINDSTED® CITREM SP70 MB (CAS number 97593–31−2) (Product code 172734), a citric acid ester of mono-diglyceride (E 472c) made from edible, refined sunflower and palm-based oil, was procured by Danisco. This product also contains α-tocopherol (E 307) max. 300 ppm and ascorbyl palmitate (E 304) max. 300 ppm.

Sodium stearoyl lactate with a purity of 97% (CAS Number: 25383-99 ID="MN1">−7) was purchased from Indagoo.

Preparation of the Chitin Particles

Chitin particles were synthesized as previously reported [21]. Briefly, 20 g of chitin (from shrimp shells, Merck) were placed in a flask with 600 mL of 3 M HCl and heated at 100 °C for 90 min under magnetic stirring. The resulting product was dialyzed in water for at least three days, centrifuged several times, and lyophilized for three days. The obtained particles presented a rod-like morphology with a length of 123 ± 16 nm.

Preparation of the Films

Firstly, Ecovio® pellets were dried in an oven for 24 h at 55 °C. Subsequently, Ecovio® pellets were mixed with the plasticizer at 10% in a beaker before being fed into the extruder. The Ecovio® blends were prepared using a Brabender MetaStation 16 extruder equipped with a double co-rotating screw (L/D 40). The temperature profile across zones 1 to 7 was set at 170/170/170/170/160/160°C, with a screw speed of 25 rpm to produce the extruded materials.

The extruded filaments were cooled in a water bath at room temperature and subsequently cut into pellets using an automatic knife cutter. The granules were then dried at 60 °C before being mixed with the particles. Xplore MC 15HT Micro Extruder instrument equipped with two conical co-rotating screws was used to mix the pellets and particles at a temperature of 165 °C and a screw speed of 40 rpm, the blend remained in the extruder for a residence time of 3 min.

For the production of thin films and to facilitate the collection of samples through the roll system, the nozzle was set to a temperature of 155 °C, along with an air system that helps cool the polymer as it exits. Three rolls were placed 25 cm apart with the following velocity profile of 300/350/30 rpm.

Antimicrobial Test

The antibacterial properties of the obtained films were tested using the E2149-20 standard method from the American Society for Testing and Materials (ASTM), a standardized method to evaluate the antimicrobial activity of material in contact with the bacteria [22]. Food pathogens *Escherichia coli* (ATCC 25922:), *Staphylococcus aureus* (ATCC 29213), as well as *Listeria innocua* (ATCC 33090) were used as bacterial strains. In this analysis, bacterial suspension was prepared in PBS. Then, 100 mg of each biopolymeric films were placed inside sterile Falcon tubes containing 1 mL of a bacterial suspension and 9 mL of PBS. Blank experiments with only the inoculum in the absence of film were also performed. Subsequently, tubes were incubated for 24 h at 37 °C with shaking at 120 rpm. The number of bacteria remaining in each sample was determined by the plate count method. The measurements were made at least in triplicate.

Results were expressed as the difference in logarithm between the initial colony formed units (CFU) concentration and the result after 24 h of suspension of the film inside the bacterial solution, following the next equation:

$$\Delta\, Log\, CFU/mL = Log\, CFU/mL\,(blank) - Log\, CFU/mL\,(after\ 24\ h) \quad (1)$$

Antioxidant Assay

The antioxidant properties of the films were evaluated employing the Blois method using the 2,2-diphenyl-1-picrylhydrazyl (DPPH, Merck) free radical. For this test, a DPPH solution was prepared by dissolving 24 mg of DPPH in 100 mL of methanol (Scharlau). For each test, 50 mg of each sample and 2 mL of the DPPH solution were added to vials, provoking the reaction. At different time periods, 100 µL of each mixture were withdrawn and transferred to a multi-well plate. The absorbance in each well was measured at 527 nm using a BioTek® SYNERGY HTX multi-mode reader spectrophotometer. After each measurement, the aliquots were returned to the original vials to maintain consistent concentration and volume. Measurements were taken at 1, 2, 3, 4, 5, 7, and 24 h.

Antioxidant capacity was determined relative to Trolox, (Thermo Scientific 97% CAS: 53188-07 ID="MN2">−1), used as the reference antioxidant. Results obtained at 24 h were expressed as Trolox equivalent antioxidant capacity (TEAC). All measurements were performed in triplicate. The following equations were employed to determine the TEAC values:

$$\mathrm{RSA}\ (\%) = 1 - \left(\frac{\Delta\ \mathrm{Absorbance\ of\ sample}}{\Delta\ Absorbance\ of\ \ control} \times 100 \right) \quad (2)$$

$$\mathrm{CTE}\ (\mu\ \mathrm{g/mL}) = (\mathrm{RSA})\ /\mathrm{mcal} \quad (3)$$

$$\mathrm{TEAC}\ (\mu\ \mathrm{mol/mg}) = (\mathrm{CTE}\ /\ \mathrm{MTrolox})/\ \mathrm{Csample} \quad (4)$$

In the equations, RSA is the radical scavenging activity, CTE denotes the Trolox equivalent coefficient, m_{cal} is the slope of the calibration curve, M_{Trolox} is the molecular weight of Trolox, and C_{sample} refers to the concentration of the sample in the DPPH solution.

Analysis of the Migrated Substances

The potential migration of the plasticizers from the packaged into food was evaluated through a migration test performed at 20 °C for 10 days, following the recommendation of the European Union and FDA recommendations (modified from the method of Yang [23]). Tests were carried out using standardized food simulants D1 (10% ethanol), D2 (3% acetic acid) and D4 (50% ethanol).

For this assay, 2 × 2 cm^2 squares of each film sample were immersed in 10 mL of each simulant and subjected to agitation for 10 days at 20 °C to simulate storage conditions of foods. Films were then extracted, dried, and weighed, while the liquid in which the films were immersed was slowly evaporated in an oven. Once the vials were dried, dichloromethane was used to dissolved the remaining residues in the vials. The extracted residues were analysed using an Agilent 8860 GC gas chromatograph equipped with an Agilent mass spectrometry detector model 5977B (GC–MS). The separation of the compounds was performed on a HP-5MS capillary column (15 m length × 250 µm internal diameter and 0.10 µm film thickness). The carrier gas used was helium with a flow rate of 1 mL/min. A volume of 1 µL of the obtained extract was injected in split mode with a split ratio of 20:1. Injector temperature was 260 °C. Compound identification was achieved by matching with the NIST 20 MS library.

Differential Scanning Calorimetry (DSC)

The thermal transitions of the Ecovio® based blends were analysed using a TA Q2000 differential scanning calorimeter (TA Instruments, New Castle, DE, USA). A nitrogen purge gas (50 cm^3/min) was applied throughout the experiments. The samples were initially heated from 20 °C to 65 °C at a rate of 10 °C/min to revert the effect of physical aging, followed by rapid cooling from 65 °C to −80 °C. A second heating scan was performed from −80 °C to 180 °C at 10 °C/min, followed by another rapid cooling, a third heating scan from −80 °C to 180 °C was conducted.

From the resulting DSC curves, the glass transition temperature (T_g), cold crystallization temperature (T_{cc}), and melting temperature (T_m) were determined. The degree of crystallinity (X_c) was calculated using the melting enthalpy values for 100% ($\Delta H_m°$) crystalline PLA (93.6 J/g) [24] and PBAT (114 J/g) and the weight fraction (W *f*) of PLA/PBAT [25].

$$Xc\ (\%) = \frac{\Delta\ Hm - \Delta\ Hcc}{\Delta\ Hm° \times\ Wf} \times\ 100 \quad (5)$$

Thermogravimetric Analysis (TGA)

Thermogravimetric analysis (TGA) was performed to evaluate the thermal stability of the various blends. Approximately 5 mg of each sample was analysed using a TGA Q500 thermal analyser (TA Instruments, New Castle, DE, USA). The samples were heated at a rate of 10 °C/min from room temperature (~30 °C) to 800 °C under an air atmosphere (50 cm^3/min). From the resulting thermograms, the temperatures corresponding to 10% (T_{d10}) and 50% (T_{d50}) mass loss were determined. Additionally, the temperature at the maximum degradation rate (T_{dmax}) was identified from the first derivative of the TGA curves (DTG).

Fourier Transform Infrared Spectroscopy (FTIR)

The FTIR spectra of the films were measured using a Perkin Elmer Spectrum Two instrument (Perkin Elmer, Waltham, MA, USA) equipped with an attenuated total reflection (ATR) module.

Confocal Raman Microscopy

To evaluate the miscibility and compatibility between different components of the films, a cryogenic fracture was performed, and the cross-section was analysed by confocal Raman microscopy on a CRM-Alpha 300 RA microscope (WITec, Ulm, Germany) equipped with Nd: YAG laser (maximum power output of 50 mW at 532 nm) and an optical resolution of approximately 250 nm in the longitudinal and 700 nm in the transversal direction. The reflected laser light at each point was collected using a multimode optical fiber of 25 µm in diameter equipped with a very sensitive CCD detector. The acquired Raman spectra were analysed by using Witec Project 2.02 program and Witec Control Plus Software.

X-ray Diffraction

The diffraction patterns of Ecovio® functionalized films were analysed using wide-angle X-ray scattering (WAXS). Measurements were conducted on a SAXSpoint 5.0 system (Anton Paar), equipped with a Cu Kα microfocus source (λ = 1.5418 Å) and a two-dimensional Pilatus 1 M detector (Dectris). This setup enables the investigation of preferred orientations in the formation of polymer crystals. The 2D X-ray diffractograms were radially integrated to generate 1D diffractograms using the SAXS Analysis software (Version 4.30.0.148 Release) provided by Anton Paar.

Mechanical Properties

Tensile testing was performed using a DX2000 QTest Elite MTS dynamometer (MTS Systems) at room temperature. The test was conducted at a stretching rate of 10 mm/min with a 100 N load cell. Dumbbell-shaped specimens were used, with a thickness of approximately 200 µm, a total length of 35 ± 0.5 mm, end width of 6 ± 0.5 mm, a narrow section length of 12 ± 0.5 mm, and a narrow section width of 2 ± 0.1 mm. Stress-strain measurements were used to calculate the ultimate tensile strength, Young's modulus, and elongation at break values.

The test was conducted in the horizontal (parallel to film orientation during calendering) and transversal directions (perpendicular to film orientation during calendering). A minimum of five specimens were tested for each material and orientation to ensure reliability.

Field Emission Scanning Electron Microscopy (FE-SEM)

Surface and cross-section microstructure of the films was analysed using a Su 8000 Hitachi FE-SEM microscopy to evaluate the distribution and compatibility of PLA and PBAT phases. To observe the cross-section of the films, a cryogenic fracture was induced by immersing the samples in liquid nitrogen.

Permeability Test

The films were cut into a circular shape (2.01 cm^2) and used to analyse water vapour and oxygen permeability using an isostatic permeability analyser (Multiperm, PERMTECH S.r.l., Pieve Fosciana, Italy) following ASTM standard methods D-3985 and F-1249, respectively. The water vapour transmission rate (WVTR) was evaluated at 23 °C and 65% relative humidity (RH), while oxygen transmission rate (OTR) measurements were monitored at 23 °C under 50% RH. Two specimens were tested for each material.

Disintegration Test

The disintegration of the films under composting were incubated following the ISO20200 standard. The solid residue for composting was prepared by manually mixing with the following composition: 55 wt% water and 45 wt% of solid waste, which consist of 10% compost (Compo®, Spain), 30% rabbit food, 10% starch, 5% sugar, 4% corn oil, 1% urea, and 40% sawdust. Two specimens were tested for each material.

Several films, each measuring 20 mm × 20 mm, were placed in textile mesh bags. These mesh bags containing the square films were then buried in the composting reactor at 58 °C under thermophilic conditions (pH 5–8).

Samples of each formulation were extracted at different incubation times for analysis. Before analysis, the samples were gently cleaned to remove adhered compost residues and then dried under vacuum at 60 °C for 24 h. The degree of disintegration was evaluated either visually and by Raman confocal microscopy using the conditions described in Section Fourier Transform Infrared Spectroscopy (FTIR).

Statistical Analysis

A one-way analysis of variance (ANOVA) followed by Tukey's post-hoc test was performed to identify significant differences ($P \leq 0.05$) among the groups.

Results and Discussion

Preparation of Functionalized Ecovio® Based Films

Functionalized Ecovio® films were prepared by a melt extrusion process followed by calendering to obtain thin films (Fig. 1). Films contained 10 wt% of the bioplasticizers and 5 wt% of either CP or SL. Table 1 shows the composition of the different composites obtained using the nomenclature ECOXXYY, where XX is referred to the bioplasticizer (SOFT-NSAFE, SS; LR 10, LR; SP70 MB, SP) and YY is referred to the additives (Sodium stearoyl lactate, SL, and chitin particles, CP). Films of approximately 200 µm of thickness were obtained.

To evaluate the composition of the films, FTIR spectroscopy was performed (Figure S1). In all the films bands associated to PLA and PBAT are clearly observed, for instance PLA/PBAT blends, for instance, carbonyl stretching vibrations of PLA and PBAT are reported at approximately at 1730 cm^{-1} and 1710 cm^{-1} for PLA and PBAT and the absorption band at 720 cm^{-1} attributed to the external bending vibration of the (–C–H) group on the benzene ring of PBAT [12]. However, with incorporation of plasticizers, CP

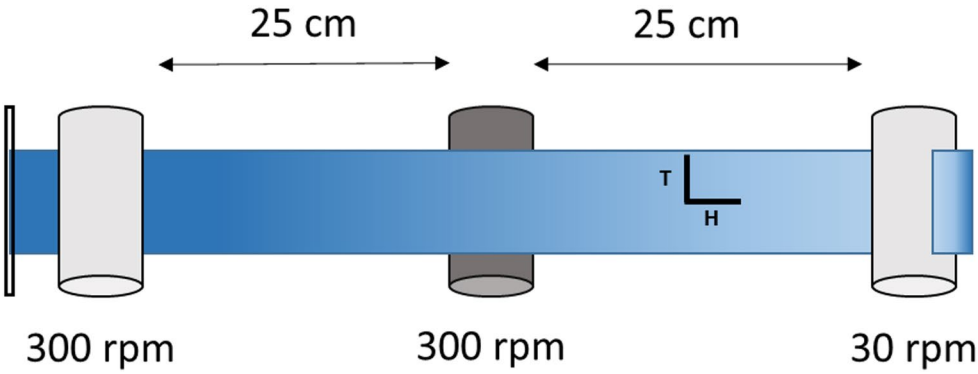

Fig. 1 Schematic of the calendered roll system and the principal direction H and the transversal T

Table 1 Composition of the prepared samples

Sample	Polymer	Plasticizer (10%)	Additive (5%)
ECO	PLA/PBAT	-	-
ECOSS	PLA/PBAT	SOFT-NSAFE	-
ECOSSSL	PLA/PBAT	SOFT-NSAFE	SL
ECOSSCP	PLA/PBAT	SOFT-NSAFE	CP
ECOLR	PLA/PBAT	LR 10	-
ECOLRSL	PLA/PBAT	LR 10	SL
ECOLRCP	PLA/PBAT	LR 10	CP
ECOSP	PLA/PBAT	SP70 MB	-
ECOSPSL	PLA/PBAT	SP70 MB	SL
ECOSPCP	PLA/PBAT	SP70 MB	CP

and SL additive, not significant changes in the spectra can be observed, probably due to the overlap of bands. Nevertheless, the analysis revealed that, for the SL samples, a new absorption band appeared at 1594 cm^{-1}, which corresponds to the carbonyl (C = O) stretching vibration from R–CO_2 groups.

Evaluation of the Thermal Properties of the Films

Thermal analysis of the prepared films was carried out to evaluate the thermal stability, crystallinity and thermal transitions, being crucial these parameters for the future applications. TGA and DTGA curves of the Ecovio® based samples were displayed in Figure S2 and Figure S3 of the Supporting Information and the thermal parameters are summarized in Table 2.

A three-step degradation process was observed in the samples, first step is associated to the PLA while the second and third are associated to the PBAT [8]. The addition of plasticizer almost does not affect the value of T_{d10}, whereas the addition of additives produced a variation in T_{d10}. CP particles produced a slightly increase in the thermal stability probably due to the formation of hydrogen bonds between chitin and polymer; contrary, SL decreases the value probably due to the degradation of SL. On the other hand, the value of T_{d50} slightly increased with the functionalization of Ecovio®. In general, the addition of both plasticizers and CP preserved a degradation mechanism similar to that of neat Ecovio® without causing notable changes in the derivative weight loss with temperature, while the presence of SL altered the degradation behaviour. Specifically, the derivative weight loss in the first step decreased, while it increased in the third step. As shown in Figure S4, the degradation of SL starts at lower temperatures than $T_{dmax}{}^1$ of the samples, the degraded products of SL could affect degradation reactions of the biopolymers such as intermolecular transesterification reactions and depolymerisation [26].

Next, DSC was employed to examine the thermal transitions and crystallization behaviour of the prepared films. Table 3 presents the values obtained from the DSC thermograms of the Ecovio® samples during the second heating

Table 2 TGA and DTGA characterization for Ecovio® samples

Sample	T_{d10} (ºC)	T_{d50} (ºC)	$T_{dmax}{}^1$ (ºC)	Der. weight[1] (%/ºC)	$T_{dmax}{}^2$ (ºC)	Der. Weight[2] (%/ºC)	$T_{dmax}{}^3$ (ºC)	Der. weight [3] (%/ºC)
ECO	330	371	345	0.013	385	0.012	466	0.006
ECOSS	326	379	343	0.013	385	0.013	455	0.002
ECOSSSL	282	381	285	0.003	389	0.018	438	0.016
ECOSSCP	339	378	353	0.009	389	0.015	481	0.009
ECOLR	333	375	344	0.011	383	0.012	460	0.003
ECOLRSL	289	390	287	0.003	397	0.020	441	0.016
ECOLRCP	335	378	350	0.011	388	0.014	460	0.003
ECOSP	330	375	349	0.007	388	0.014	457	0.009
ECOSPSL	281	384	284	0.003	389	0.015	436	0.018
ECOSPCP	335	382	349	0.012	392	0.014	464	0.002

Table 3 Thermal parameters obtained from the second heating DSC curves of Ecovio® based films: glass transition temperature (T_g), melting temperature (T_m) and degree of crystallinity (X_c)

Sample	T_g^{PBAT} (ºC)	T_g^{PLA} (ºC)	T_m^{PBAT} (ºC)	T_m^{PLA} (ºC)	X_c^{PBAT} (%)	X_c^{PLA} (%)
ECO	−32	59	123	149	6.6	6.1
ECOSS	−30	53	117	150	8.5	5.8
ECOSSSL	−32	54	116	151	10.2	6.4
ECOSSCP	−33	51	117	150	10.9	6.3
ECOLR	−32	58	123	147	6.6	7.3
ECOLRSL	−32	56	120	152	10	9.3
ECOLRCP	−32	60	125	148	3.5	5.6
ECOSP	−32	59	122	145	6.5	6.5
ECOSPSL	−31	58	122	151	7.4	9.2
ECOSPCP	−32	59	123	150	6.9	4.7

scan, conducted from − 80 °C to 180 °C. The initial heating up to 65 °C was specifically performed to eliminate the effects of physical aging, a phenomenon commonly observed in PLA-based materials due to their glass transition temperatures (T_g) being relatively close to room temperature. The DSC thermograms exhibited two glass transitions, the first one attributed to PBAT at lower temperatures and the second attributed to PLA at higher temperatures. This behaviour indicates the non-miscibility between these two polymers as previously reported [13, 27].

In the Ecovio® samples with the plasticizer SOFTNSAFE, the value of the T_g of PLA is reduced, as a result of the plasticisation effect of the bioplasticizers, resulting in an increase in the mobility of the polymer chains, while the T_g of PBAT is not modified practically with the addition of the plasticizer [28]. Besides, melting temperature (T_m) of PBAT is slightly reduced with the addition of this plasticizer. The plasticizer does not vary the crystallinity of the PLA and PBAT phase in comparison with the ECO neat film, while the addition of the SL additive increases the crystallinity of the PBAT and PLA phases. This behaviour could be explained due to the good distribution of the additive which can act as a nucleating agent increasing the crystallinity. Likewise, the addition of CP in ECOSSCP slightly increases the crystallinity of both phases. In the rest of the films with the other bioplasticizers the thermal parameters do not noticeably vary with the incorporation of any component.

Characterization of the Structural, Mechanical and Permeability Properties of the Films

Structural and Mechanical Properties

FE-SEM was employed to examine the surface morphology and the interior, after cryogenic fracturing, of the calendered samples. As shown in Fig. 2A (left image), the surface of ECO sample appears relatively homogeneous, with the PLA and PBAT phases displaying good miscibility. FE-SEM was also used to investigate the cross-section of the composites after cryogenic fracturing. The images in Fig. 2A (right image) reveal the presence of spherical domains likely originating from one of the polymers embedded within the matrix of the other, indicating phase separation at the interlayer level [13, 29], nevertheless good homogeneity is observed. Furthermore, the incorporation of SL and CP altered the cross-section morphology, introducing variations in surface roughness, as illustrated in Fig. 2B.

To further study the morphology, Raman confocal microscopy was employed to study the distribution of PLA and PBAT phases and to evaluate the dispersion of the additives, CP and SL in the Ecovio® based films.

Initially, Raman confocal microscopy was used to scan the surface of Ecovio®-based samples (see Figure S5 of Supporting Information). Although small regions or domains of PLA could be poorly distinguished from those of PBAT; however, the distribution and size of these domains could not be clearly observed due to the limited depth resolution of the Raman signal at the surface. To overcome this limitation, samples were cryo-fractured and analysed further.

Figure 3 shows as an example, Raman maps in the cross-section of the films, acquired using a 10 mW laser power and a 100× objective lens, for the samples ECOSP, ECOSPSL, and ECOSPCP

The images reveal that the PLA phase (indicated in blue) is homogeneously distributed in quasi-spherical microdomains throughout the PBAT matrix (shown in pink). These microdomains are also smaller in size than the segregated domains obtained in previous publications in which the Ecovio® based films were produced by compression moulding [12], indicating a better mixing process between both polymeric phases. Furthermore, SL (shown in red) appears to be homogeneously distributed in the interfacial regions, forming microdomains within the polymer matrix. In contrast, CP exhibited a less homogeneous distribution, forming domains of different sizes (represented in cyan). Similar results were observed for the rest of the films.

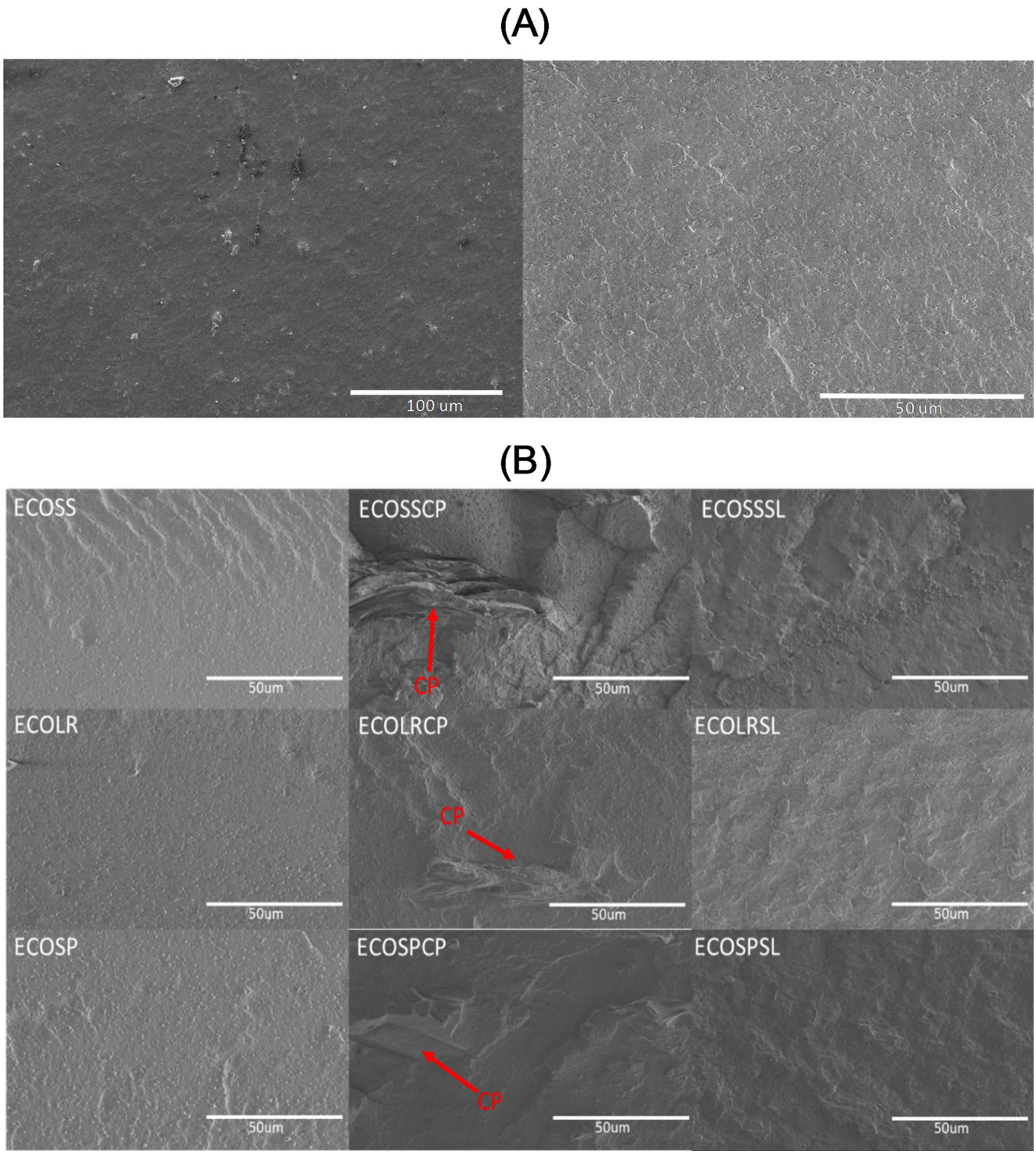

Fig. 2 FE-SEM images of (**A**) ECO sample showing the surface morphology (left) and cross-section (right), and (**B**) cross-section images with a 1000x magnification of the prepared films containing the bioplasticizers and the additives

The mechanical parameters derived from the stress-strain curves obtained during the tensile tests are summarized in Table 4. Remarkably, the elongation at break values for the calendered samples show a significant improvement compared to the functionalized Ecovio® samples produced by compression moulding recently published [12], probably due to the better mixing process, which give smaller microdomains of PLA homogeneously distributed within the PBAT matrix. In general, no notable increase in elongation at break was observed with the incorporation of the

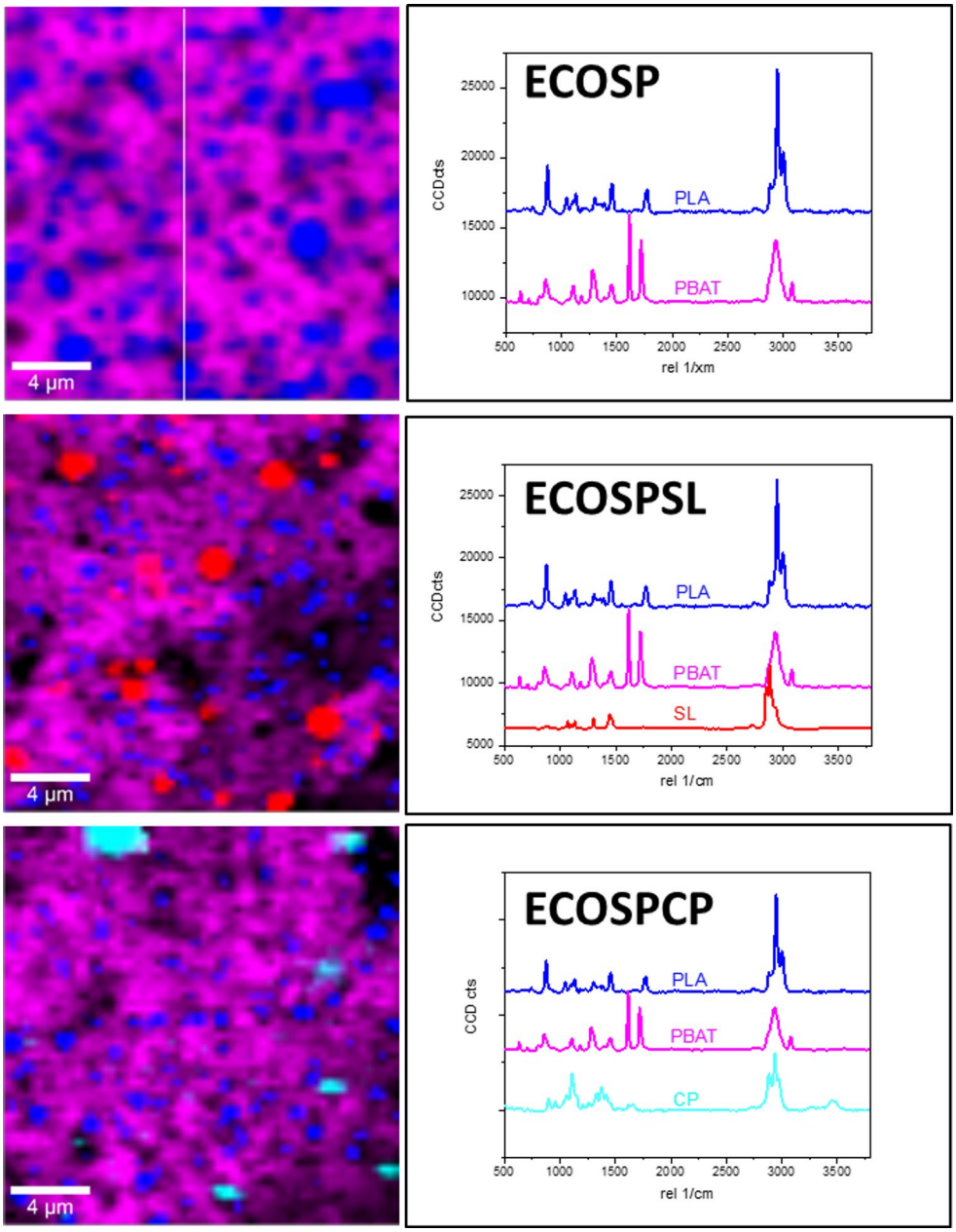

Fig. 3 Raman spectra of ECOSP, ECOSPSL and ECOSPCP (right). XY Raman images of ECOSP, ECOSPSL and ECOSPCP matrix (left) where PBAT was signalled in pink, PLA was signalled in blue and SL and CP particles were signalled in red, and cyan, respectively.

plasticizers; nonetheless, the values of Young's modulus and ultimate stress were slightly reduced. This suggests that the used bioplasticizers do not provide additional plasticizing effects beyond those already achieved by the good blending of the two polymeric phases, PLA and PBAT. Another significant differences in calendered films in comparison with the films produced by compression moulding is the introduction of anisotropy, which affects the mechanical behaviour of films, evident in the parallel (H) and transverse (T) directions. In this case, this anisotropy is, however, not significant in ECO, ECOLR, ECOSS and ECOSP films. Only the incorporation of SL additives provokes significant differences in the mechanical properties between the two directions. The addition of SL particles produces a high anisotropy between the H and T direction resulting in higher elongation at break in the H direction and lower in the T direction. A similar trend is observed in the ultimate tensile strength and Young's modulus. As reported in the literature for oriented PLA/PBAT films containing fillers, the addition of particles produces anisotropy. This is due to molecular orientation that occurs during processing [30, 31]. Moreover, another explanation is that additives added into the polymeric matrix can agglomerate and result as stress concentrators points that produce an early failure of the composite [32]. On the other hand, the incorporation of CP particles leads to an overall deterioration of mechanical

Table 4 Mechanical properties of the functionalized films

Sample	Ultimate Stress (MPa)	Young Modulus (MPa)	Elongation at break (%)
ECO H	24.4 ± 4.2^{a}	179.2 ± 7.8^{b}	490.2 ± 91.1^{ab}
ECO T	25.7 ± 1.6^{a}	135.2 ± 4.8^{cdef}	542.8 ± 36.2^{ab}
ECOSS H	21.3 ± 2.1^{abc}	109.7 ± 0.5^{fg}	478.1 ± 50.4^{abc}
ECOSS T	21.6 ± 1.4^{abc}	95.7 ± 7.5^{g}	530.6 ± 67.7^{ab}
ECOSSSL H	22.0 ± 0.8^{ab}	154.0 ± 10.1^{bcd}	587.3 ± 15.3^{a}
ECOSSSL T	12.5 ± 0.8^{g}	119.8 ± 8.6^{defg}	298.3 ± 32.6^{ef}
ECOSSCP H	18.1 ± 0.5^{bcde}	123.8 ± 12.6^{defg}	397.4 ± 18.4^{bcde}
ECOSSCP T	13.3 ± 1.4^{efg}	112.7 ± 2.6^{efg}	296.3 ± 60.6^{def}
ECOLR H	22.2 ± 1.4^{ab}	120.4 ± 4.5^{defg}	518.8 ± 37.6^{ab}
ECOLR T	22.6 ± 0.9^{ab}	136.3 ± 3.8^{cdefg}	515.5 ± 17.7^{ab}
ECOLRSL H	19.3 ± 0.7^{bcd}	225.0 ± 18.0^{a}	449.10 ± 70.2^{abcd}
ECOLRSL T	11.0 ± 0.8^{g}	128.4 ± 4.4^{defg}	259.8 ± 44.8^{ef}
ECOLRCP H	14.8 ± 0.7^{defg}	142.3 ± 4.0^{cdef}	282.8 ± 29.8^{ef}
ECOLRCP T	12.8 ± 1.0^{fg}	134.5 ± 5.4^{cdefg}	217.5 ± 27.5^{f}
ECOSP H	21.9 ± 0.9^{ab}	162.3 ± 4.0^{bc}	473.1 ± 64.1^{ab}
ECOSP T	21.5 ± 2.0^{abc}	138.0 ± 9.6^{cdef}	510.2 ± 67.8^{ab}
ECOSPSL H	19.9 ± 2.4^{bc}	182.6 ± 29.1^{b}	450.6 ± 8.2^{abcd}
ECOSPSL T	12.2 ± 0.7^{g}	138.8 ± 16.0^{cdef}	248.1 ± 22.6^{ef}
ECOSPCP H	17.2 ± 0.7^{cdef}	149.8 ± 4.0^{bcde}	333.8 ± 18.1^{cdef}
ECOSPCP T	14.2 ± 1.4^{efg}	138.6 ± 10.4^{cdef}	273.3 ± 34.0^{f}

Values having the same letter are not significantly different for Tukey test (significance level of $P \leq 0.05$)

properties in both directions [33, 34] due to the big size and/or their aggregation.

To better understand the influence of the parallel and transverse stretching directions on the mechanical properties, especially in the films containing SL additives, X-ray diffraction analyses were conducted in both orientations, specifically, Wide-Angle X-ray Scattering (WAXS).

As shown in Fig. 4, when comparing the crystallinity based on the halos obtained by WAXS, no significant differences are observed. This indicates that the crystallinity is similar in both the transverse and parallel directions. This result is also confirmed in Fig. 4 **and** Figure S6, where the WAXS diffractograms for both directions are presented and exhibited no significant differences between both directions. Nevertheless, the overall degree of crystallinity is very low. This low crystallinity is attributed to the inherently slow crystallization rate of PLA. When PLA is stretched, it primarily promotes orientation within the amorphous phase rather than increasing crystallinity [35–37]. This orientation of the amorphous phase might be responsible for the observed anisotropy in the mechanical properties rather than differences in the crystalline structure.

Permeability of the Films

Water vapour and oxygen permeabilities are also critical properties in assessing biobased food packaging films [38]. Permeance refers to the transmission rate of a substance through a film divided by the partial pressure difference whereas across it, while permeability is obtained by multiplying the permeance by the film thickness [39]. Figure 5 shows the water vapour (KP_{WV}) and oxygen (KP_{O2}) permeability values. Compared with the ECO sample, both KP_{WV} and KP_{O2} decreased with the addition of plasticizers, SL and CP, that could be attributed to the increased interaction between the additives and the polymer chains, which decreased the free channel for the transit of water vaper and oxygen. Nevertheless, when expressed as logarithmic values (Log WVP for water vapour and Log O_2P for oxygen), the results showed no significant change from ECO sample. The films displayed high permeability, with Log WVP values ranging from approximately 5.3 to 5.6 and Log O_2P values from 4.6 to 4.8, suggesting potential suitability for applications requiring high gas transmission, as packaging for bakery products, fruits, salads, or vegetables [39, 40].

Antioxidant and Antimicrobial Assays

After confirming the effects of plasticizers and particles on the thermal and mechanical properties of the films, their antioxidant and antibacterial activities were further evaluated. Table 5 presents the values of CTE and TEAC after 24 h of exposure to DPPH solutions. The functionalized Ecovio® samples exhibited antioxidant activity, in contrast to the neat Ecovio®, which showed a TEAC value of 3.20 ± 0.49 µmol Trolox/g. Functionalization with the bioplasticizers drastically increased antioxidant capacity by a factor of approximately 10, while the incorporation of CP enhances a bit more the antioxidant activity. It has been previously reported that chitin nanocrystals can provide certain antioxidant activity to polymeric films [41], although the biggest contribution is due to the bioplasticizers ACETEM and CITREM. Among the functionalized films, ECOSPCP exhibited the highest TEAC value at 18.58 ± 0.48 µmol Trolox/g, followed by ECOLRCP with 17.54 ± 0.24 µmol Trolox/g, values much higher than others found in literature for polyolefins films used in packaging, which were able to prevent oxidation reaction in food [42]. When comparing films within the same plasticizer series, the addition of CP additive consistently enhanced the TEAC values, this antioxidant action of chitin particles is attributed to their hydroxyl and amino groups of their structures, which are able to donate hydrogen to free radicals [41]. Therefore, the results revealed the potential of these functionalized films as antioxidant active packaging.

Next, the antimicrobial properties of the films containing plasticizers were evaluated using a film contact method against *Escherichia coli*, *Staphylococcus aureus* and *Listeria innocua* bacteria. Samples did not exhibit antibacterial

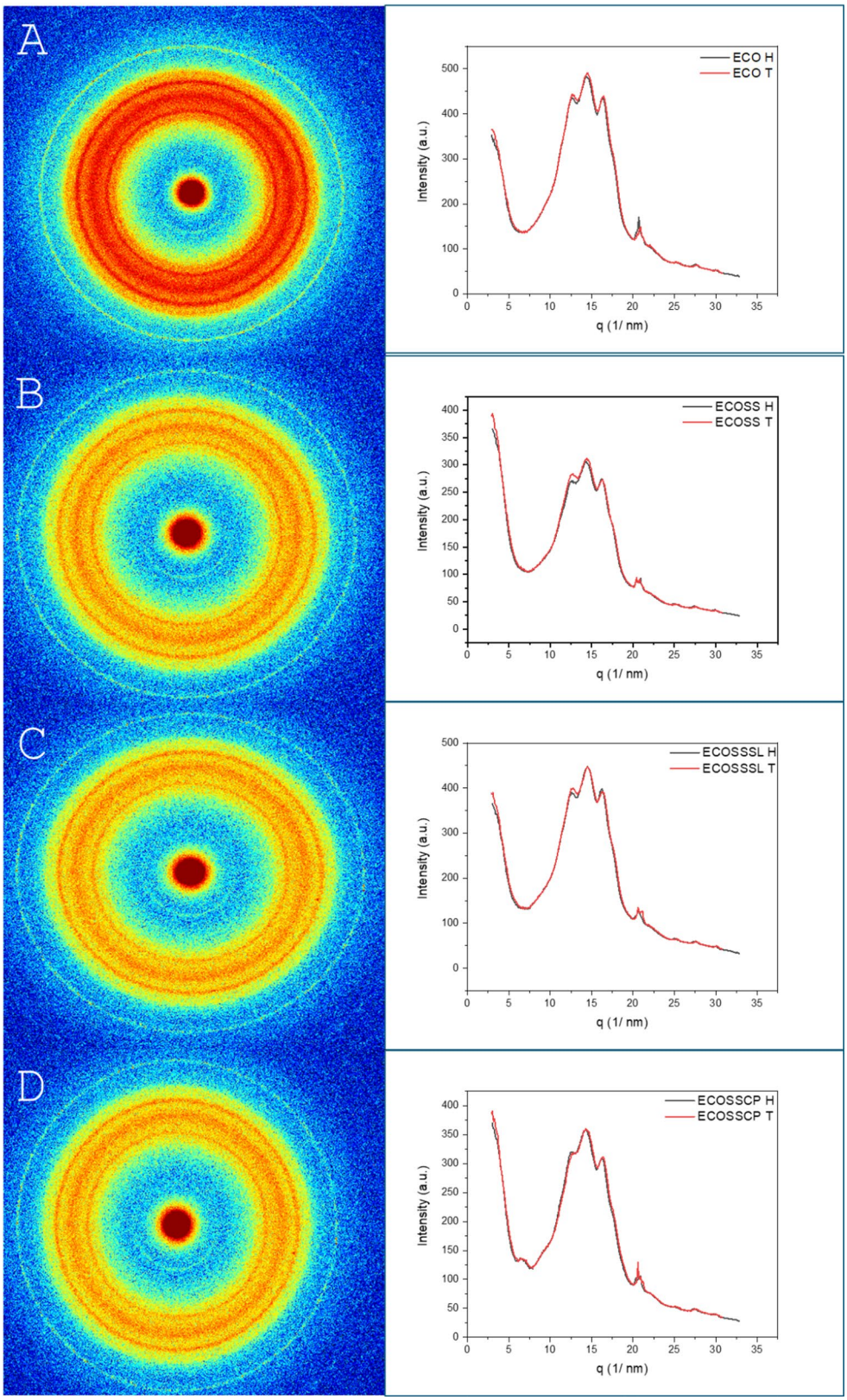

Fig. 4 WAXS images and diffractograms in 1D of (**A**) ECO, (**B**) ECOSS, (**C**) ECOSSSL, (**D**) ECOSSCP

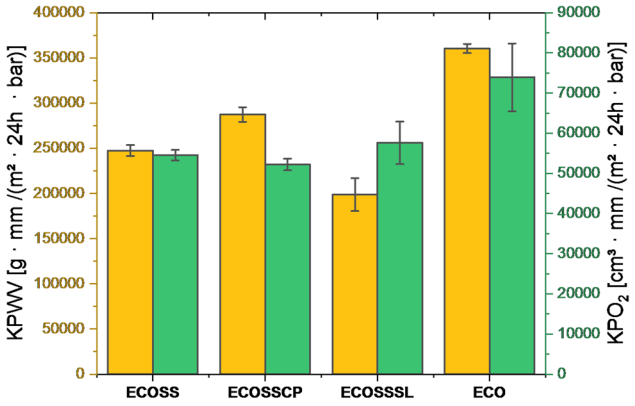

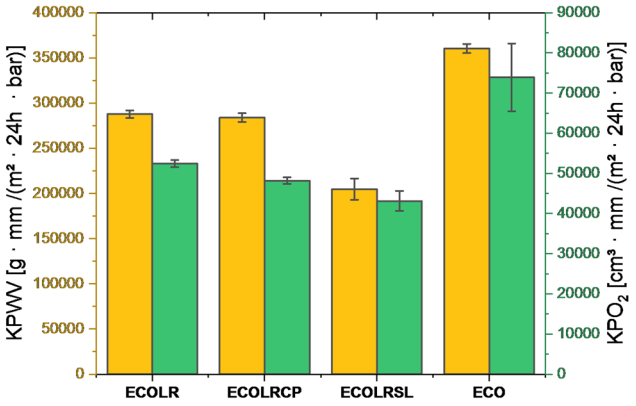

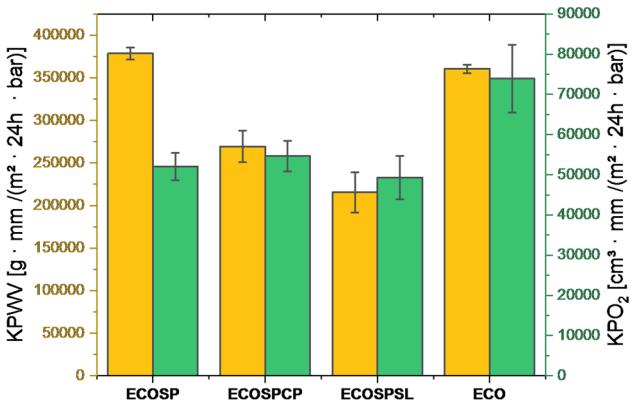

Sample	Log(WVP)	Log(O_2P)
ECO	5.56	4.87
ECOSS	5.39	4.74
ECOSSSL	5.30	4.76
ECOSSCP	5.46	4.72
ECOLR	5.46	4.72
ECOLRSL	5.31	4.63
ECOLRCP	5.45	4.68
ECOSP	5.58	4.72
ECOSPSL	5.33	4.69
ECOSPCP	5.43	4.74

Fig. 5 KP_{WV} and KP_{O2} value for Ecovio® based materials and Table of the values of Log WVP and Log O_2P

Table 5 Antioxidant properties of the functionalized films

Sample	CTE (µg Trolox/mL)	TEAC (µmol Trolox/g)
ECO	4.00±0.61	3.20±0.49^{a}
ECOSS	17.79±0.50	14.21±0.40^{b}
ECOSSSL	18.79±0.65	15.02±0.52^{b}
ECOSSCP	19.43±0.30	15.53±0.24^{b}
ECOLR	16.52±0.35	13.20±0.28^{bc}
ECOLRSL	17.87±0.73	14.27±0.58^{b}
ECOLRCP	21.95±0.30	17.54±0.24^{d}
ECOSP	18.31±0.35	14.63±0.28^{b}
ECOSPSL	21.00±0.12	16.79±0.10^{bc}
ECOSPCP	23.26±0.60	18.58±0.48^{d}

Values having the same letter are not significantly different for Tukey test (significance level of $P \leq 0.05$)

activity against the Gram-negative *Escherichia coli*, due to the double lipid bilayer membrane that limits the penetration of antimicrobial compounds. Table 6 presents the antibacterial activity of the tested materials against the two Gram-positive strains, expressed as the log reduction in bacterial count after 24 h of contact with the films. Examples of the agar plate images used to determine the bacterial

Table 6 Antimicrobial properties against *S. aureus* (initial inoculum 4.54±0.01 log CFU/mL) and *L. innocua* (initial inoculum 3.71±0.04 log CFU/mL).

Sample	S. aureus (ΔLog CFU/mL)	L. innocua (ΔLog CFU/mL)
ECOSS	0.63±0.06^{b}	0.42±0.01^{b}
ECOSSSL	4.54±0.01^{a}	3.71±0.04^{a}
ECOSSCP	0.11±0.01^{b}	0.10±0.03^{c}
ECOLR	4.54±0.01^{a}	2.30±004^{d}
ECOLRSL	4.54±0.01^{a}	3.71±0.04^{a}
ECOLRCP	4.54±0.01^{a}	1.76±0.27^{e}
ECOSP	4.54±0.01^{a}	3.71±0.04^{a}
ECOSPSL	4.54±0.01^{a}	3.71±0.04^{a}
ECOSPCP	4.54±0.01^{a}	3.71±0.04^{a}

Values having the same letter are not significantly different for Tukey test (significance level of $P \leq 0.05$)

reduction percentage are depicted in Figure S8 (Supporting information). The initial inoculum concentrations were 4.54±0.01 log CFU/mL for *S. aureus* and 3.71±0.04 log CFU/mL for *L. innocua*. As regards *S. aureus*, total inhibition was observed in most of the samples, except for

ECOSS and ECOSSCP, which showed minimal bacterial reduction counts of 0.63 ± 0.06 log CFU/mL and 0.11 ± 0.01 log CFU/mL, respectively. These results highlight the antimicrobial activity of SL, which allowed for a total bacterial inhibition when using the ECOSSSL sample. Additionally, SL and CP in CITREM containing samples did not produce any antagonistic effects, as antimicrobial activity against *S. aureus* was maintained.

In the case of *L. innocua*, the Ecovio® samples containing CITREM SP demonstrated a complete inhibition, both with and without the addition of particles, pointing out the good antimicrobial activity of such bioplasticizer. For CITREM LR10, antimicrobial activity was evident in the ECOLR and ECOLRCP samples, with reductions of 2.30 ± 0.04 log CFU/mL and 1.76 ± 0.27 log CFU/mL, respectively, although the inhibition achieved was not complete. Notably, ECOLRSL containing SL additive showed complete inhibition. Finally, ECOSS and ECOSSCP exhibited minimal antimicrobial activity against *L. innocua*, with reductions of 0.42 ± 0.01 log CFU/mL and 0.10 ± 0.03 log CFU/mL, respectively. On the other hand, the incorporation of SL additive significantly enhanced the antimicrobial effect, resulting in total inhibition, as shown for *S. aureus*. The antimicrobial activity of the bioplasticizers CITREM LR10 and CITREM SP is presumably attributed to the germicidal effects of citric acid, which lowers the local and intracellular pH, causing damage to proteins, enzymes, DNA, and membranes, as well as suppressing NADH oxidation, ultimately leading to bacterial death [43, 44]. SL is likely able to damage bacteria through a dual mechanism: (1) its fatty acid chain disrupts bacterial membranes by integrating into the lipid bilayer, causing leakage and cell damage particularly in Gram-positive bacteria with simpler membranes [45]; and (2) its lactylate component acidifies the cytoplasm by releasing protons and lactate anions, disrupting cellular processes and consuming energy needed for growth [46]. The enhanced susceptibility of Gram-positive bacteria to SL further supports this dual mechanism, as their limited membrane defences render them more vulnerable to both membrane disruption and acid stress.

Migration of the Plasticizers

Migration of plasticizers from packaging films is a persistent concern, especially for applications involving direct contact with food. Even when employing authorized additives by the FDA like sodium ACETEM (E472a) or CITREM (E472c), the migration from the packaging into the food can affect properties like flavours, aromas, among other sensorial properties.

To evaluate the migration of products, The European Commission has established directives, such as Commission Regulation (EU) No 10/2011, to define the simulants used for studying the migration of substances from materials intended to come into contact with food [47]. In this study, the extent of migration was assessed using standard food simulants: Simulant A, composed of 10% ethanol in water; simulant B containing 3% acetic acid in water; and simulant D1, composed by 50% ethanol in water. Film samples were submerged in the medium for a period of 10 days at 20 °C. After the exposure period, the films were retrieved and weighed again, while the simulant solution was subjected to complete evaporation in an oven. Across all samples, no measurable mass loss was observed in the films, suggesting minimal or negligible migration. Even if the residue was not seen by gravimetric analysis in the vial, 150 µL of DCM were employed to wash the vial and extract the possible migration products. That solution was analysed by gas chromatography–mass spectrometry (GC–MS). Prior to analysis, calibration was conducted for the key components present in each plasticizer, enabling quantification of the peaks identified in the chromatograms. In the case of samples in simulants A and B, no migration of the plasticizer was detected. However, in simulant D, some substances were detected (Table 7). The migration value of the main components were far below to the maximum specific migration limit established at 60 mg/kg$_{food}$ (restriction limit for the group of additives to which it belongs) [47].

Disintegrability of the Films Under Composting Conditions

The end-of-life study of packaging is also essential for assessing its environmental impact. Herein, the disintegradability of the prepared films in industrial composting conditions was evaluated. Figure 6 shows the degradation of the functionalized Ecovio® samples over different incubation times under composting. Samples were collected after 20, 45, 90, and 135 days to evaluate properties such as fragility and colour changes. All films showed visible disintegration during composting. During the first 20 days of incubation, the films lost their transparency and became yellowish. By day 45, the samples darkened further and exhibited fractures, indicating the onset of hydrolytic degradation of the polymer matrix. With prolonged incubation,, the degradation effects intensified, leading to the formation of holes and fragmentation into smaller pieces [48, 49].

To further understand the disintegration under composting of the composite films Raman confocal micoscopy was employed to anaylise the degraded films. Figure 7 presents, as example, the Raman images obtained for ECOSP, ECOSPSL, and ECOSPCP at different composting times. In these images, it is possible to observe that both PLA and PBAT phases coexist up to 45 days of composting. However, in the

Table 7 Results obtained from the migration study analysed by GC–MS in simulant D (50% ethanol in water)

Sample	Retention time (min)	Main component	R^2	Migration amount (mg/kg)
ECOSS	22.0	3-((12-Acetoxyoctadecanoyl)oxy)propane-1,2-diyl diacetate	0.999	0.0594
ECOSSCP	22.0	3-((12-Acetoxyoctadecanoyl)oxy)propane-1,2-diyl diacetate	0.999	0.0744
ECOSSSL	22.0	3-((12-Acetoxyoctadecanoyl)oxy)propane-1,2-diyl diacetate	0.999	0.0486
ECOLR	29.8	9-Octadecenoic acid (Z)-, 2-hydroxy-1,3-propanediyl ester	0.999	0.0132
ECOLRCP	29.8	9-Octadecenoic acid (Z)-, 2-hydroxy-1,3-propanediyl ester	0.999	0.0036
ECOLRSL	29.8	9-Octadecenoic acid (Z)-, 2-hydroxy-1,3-propanediyl ester	0.999	0.0030
ECOSP	28.7	9-Octadecenoic acid (Z)-, 2-hydroxy-3-[(1-oxohexadecyl)oxy] propyl ester	0.995	0.0594
ECOSPCP	28.7	9-Octadecenoic acid (Z)-, 2-hydroxy-3-[(1-oxohexadecyl)oxy] propyl ester	0.995	0.0072
ECOSPSL	28.7	9-Octadecenoic acid (Z)-, 2-hydroxy-3-[(1-oxohexadecyl)oxy] propyl ester	0.995	0.0072

image corresponding to 90 days, the PLA phase is no longer visible. This observation is consistent with previous studies, which have demonstrated that PLA undergoes faster disintegration under composting conditions compared to PBAT [8, 12, 50, 51]. Moreover, CP and SL particles were present in the matrix up to 20 days, but were no longer observed at 45 days. Similar behaviour was observed in the other samples exhibited in Figure S7 of Supporting Information.

These results allow us to propose the hypothesis that films degradation of the occurs in different stages. The first stage involves the disappearance of the particles, observed between 20 and 45 days, which likely generates small holes where fracture begins. Secondly, the complete disintegration of the PLA phase occurred before 90 days, then, the total degradation of PBAT take longer times. Interestingly, the incorporation of the plasticizers or the additives CP and SL did not impact on the desistegradability and degradation of the Ecovio based films, as previously reported en PLA and Ecovio based films [12, 52].

Conclusions

In summary, biodegradable Ecovio® (PLA/PBAT) films incorporating food-grade additives such as CITREM, ACETEM, sodium stearoyl lactylate and chitin particles, has resulted in promising functional materials with notable antioxidant, antimicrobial, and mechanical properties for food packaging applications. In particular and on the permeability results, the films could be applied in food products such as fruits, salads or bakery products.

The calendering process has enabled the production of uniform, high-quality films with excellent elongation at break and good additive dispersion; however, the incorporation of SL additive induces anisotropy in the mechanical properties. Besides, the thermal and barrier properties remained largely unchanged, while the films exhibited strong antimicrobial activity against key gram-positive bacteria and demonstrated effective antioxidant capacity, with minimal migration into food simulants.

Importantly, the produced films were shown to disintegrate under industrial composting conditions, confirming their potential for sustainable end-of-life management. Overall, these findings underscore the suitability of such formulations for active and environmentally friendly food packaging applications.

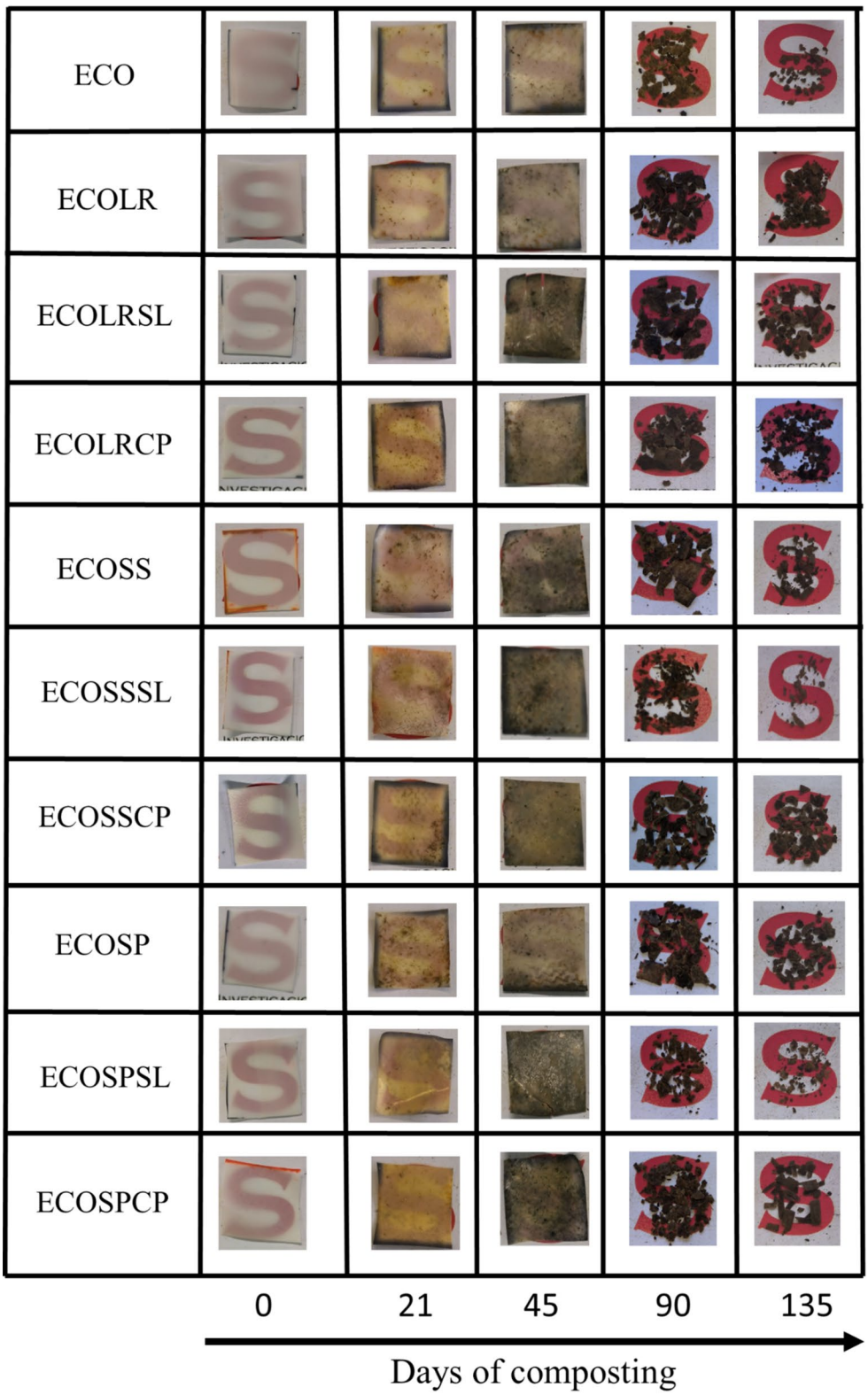

Fig. 6 Visual appearance of the tested films at different composting times. Samples were collected at 20, 45, 90, and 135 days

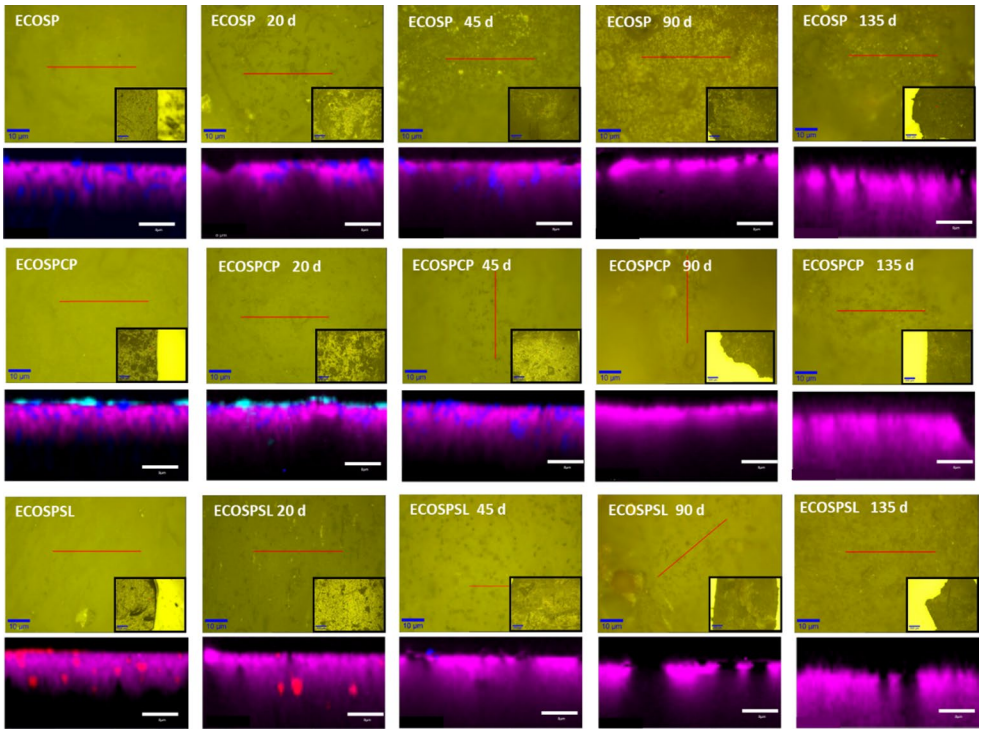

Fig. 7 Raman images of disintegration of ECOSP, ECOSPSL and ECOSPCP samples at different days under composting conditions. Scale bar of 8 µm

Supplementary Information The online version contains supplementary material available at https://doi.org/10.1007/s10924-025-03724-z.

Acknowledgements This work was funded by the EU H2020 Project, "Characterisation and Harmonisation for Industrial Standardisation of Advanced Materials" (CHARISMA), under Grant Agreement no. 952921 and by the Ministerio de Ciencia, Innovación y Universidades (PID2022-13651OB-100), the Agencia Estatal de Investigación (AEI, Spain) and Fondo Europeo de Desarrollo Regional (FEDER, EU).

Author Contributions The article was written with contributions from all authors and all authors have reviewed and approved the final version of the manuscript. I.M.P. conducted the investigation, formal analysis, and wrote the original draft. M.F.G., E.B.B., S.L., M.R., D.M.M., J.P.F.B. contributed to conceptualization, formal analysis and methodology. A.D.C. and A.M.B. contributed to conceptualization, formal analysis and methodology and conducted supervision of the work and management of the project.

Funding Open Access funding provided thanks to the CRUE-CSIC agreement with Springer Nature.

Data Availability No datasets were generated or analysed during the current study.

Declarations

Competing Interests The authors declare no competing interests.

References

1. Nuojua S, Pahl S, Thompson RC (2024) Plastic alternatives and substitutes in the packaging sector – A UK consumer perspective. Sustain Prod Consum 46:68–81. https://doi.org/10.1016/J.SPC.2024.02.019
2. European Union (2024) Regulation (EU) 2025/40 of the European Parliament and of the Council of 19 December 2024 on packaging and packaging waste, amending regulation (EU) 2019/1020 and directive (EU) 2019/904, and repealing directive 94/62/EC (Text with EEA relevance)
3. Peelman N, Ragaert P, De Meulenaer B et al (2013) Application of bioplastics for food packaging. Trends Food Sci Technol 32:128–141. https://doi.org/10.1016/j.tifs.2013.06.003
4. González-López ME, Calva-Estrada SdeJ, Gradilla-Hernández MS, Barajas-Álvarez P (2023) Current trends in biopolymers for food packaging: a review. Front Sustain Food Syst 7:1–20. https://doi.org/10.3389/fsufs.2023.1225371
5. Narancic T, Cerrone F, Beagan N, O'Connor KE (2020) Recent advances in bioplastics: application and biodegradation. Polymers. https://doi.org/10.3390/POLYM12040920
6. Marano S, Laudadio E, Minnelli C, Stipa P (2022) Tailoring the barrier properties of PLA: a state-of-the-art review for food packaging applications. Polymers. https://doi.org/10.3390/polym14081626
7. Mangaraj S, Yadav A, Bal LM et al (2019) Application of Biodegradable Polymers in Food Packaging Industry: A Comprehensive

Review. J Packag Technol Res 3:77–96. https://doi.org/10.1007/s41783-018-0049-y
8. del Campo A, de Lucas-Gil E, Rubio-Marcos F et al (2021) Accelerated disintegration of compostable Ecovio polymer by using ZnO particles as filler. Polym Degrad Stab 185:109501. https://doi.org/10.1016/j.polymdegradstab.2021.109501
9. Mena-Prado I, Fernández-García M, del Campo A, Bonilla AM (2025) Natural macromolecules used as Bioplasticizer in polymer materials for food contact applications. Packag Technol Sci 511–526. https://doi.org/10.1002/pts.2899
10. Amara S, Patin A, Giuffrida F et al (2014) In vitro digestion of citric acid esters of mono- and diglycerides (CITREM) and CITREM-containing infant formula/emulsions. Food Funct 5:1409–1421. https://doi.org/10.1039/c4fo00045e
11. Mena-Prado I, Fernández-García M, Blázquez-Blázquez E et al (2024) Plasticizing PLA with biobased fatty esters: comprehensive study on film properties. J Polym Environ. https://doi.org/10.1007/s10924-024-03454-8
12. Mena-Prado I, Navas-Ortiz E, Fernández-García M et al (2024) Enhancing functional properties of compostable materials with biobased plasticizers for potential food packaging applications. Int J Biol Macromol 135538. https://doi.org/10.1016/j.ijbiomac.2024.135538
13. Ludwiczak J, Frąckowiak S, Leluk K (2021) Study of thermal, mechanical and barrier properties of biodegradable pla/pbat films with highly oriented mmt. Materials. https://doi.org/10.3390/ma14237189
14. Faergemand M, Krog N (2003) 10 - Using emulsifiers to improve food texture. In: McKenna BMBT-T (ed) Woodhead Publishing Series in Food Science, Technology and Nutrition. Woodhead Publishing, pp 216–250
15. Garavito J, Peña-Venegas CP, Castellanos DA (2024) Production of starch-based flexible food packaging in developing countries: analysis of the processes, challenges, and requirements. Foods. https://doi.org/10.3390/foods13244096
16. Sacco F, Di, Gahleitner M, Wang J, Portale G (2020) Systematic investigation on the structure-property relationship in isotactic polypropylene films processed via cast film extrusion. Polym (Basel) 12. https://doi.org/10.3390/POLYM12081638
17. Priyadarshi R, Rhim JW (2020) Chitosan-based biodegradable functional films for food packaging applications. Innov Food Sci Emerg Technol 62:102346. https://doi.org/10.1016/j.ifset.2020.102346
18. Chang SH, Chen YJ, Tseng HJ et al (2021) Applications of nisin and edta in food packaging for improving fabricated chitosan-polylactate plastic film performance and fish fillet preservation. Membranes (Basel). https://doi.org/10.3390/membranes11110852
19. Azeredo HMCd (2009) Nanocomposites for food packaging applications. Food Res Int 42:1240–1253. https://doi.org/10.1016/j.foodres.2009.03.019
20. Tan JM, Li B, Han SY, Wu H (2023) Use of a compound modifier to retard the quality deterioration of frozen dough and its steamed bread. Food Res Int 172:113229. https://doi.org/10.1016/j.foodres.2023.113229
21. Muñoz-Núñez C, Hevilla V, Zágora J et al (2025) Functionalization of chitosan-chitin nanowhiskers films by impregnation with essential oils via supercritical CO2. J Polym Environ 33:96–111. https://doi.org/10.1007/s10924-024-03413-3
22. ASTM E2149-13 A standard test method for determining the antimicrobial activity of antimicrobial agents under dynamic contact conditions
23. Yang C, Zhu B, Wang J, Qin Y (2019) Structural changes and nano-TiO2 migration of poly(lactic acid)-based food packaging film contacting with ethanol as food simulant. Int J Biol Macromol 139:85–93. https://doi.org/10.1016/j.ijbiomac.2019.07.151
24. Badia JD, Santonja-Blasco L, Martínez-Felipe A, Ribes-Greus A (2012) Hygrothermal ageing of reprocessed polylactide. Polym Degrad Stab 97:1881–1890. https://doi.org/10.1016/j.polymdegradstab.2012.06.001
25. Herrera R, Franco L, Rodríguez-Galán A, Puiggalí J (2002) Characterization and degradation behavior of poly(butylene adipate-co-terephthalate)s. J Polym Sci Part A Polym Chem 40:4141–4157. https://doi.org/10.1002/pola.10501
26. Xiang S, Feng L, Bian X et al (2020) Evaluation of PLA content in PLA/PBAT blends using TGA. Polym Test 81:106211. https://doi.org/10.1016/j.polymertesting.2019.106211
27. Li X, Ai X, Pan H et al (2018) The morphological, mechanical, rheological, and thermal properties of PLA/PBAT blown films with chain extender. Polym Adv Technol 29:1706–1717. https://doi.org/10.1002/pat.4274
28. Lim LT, Auras R, Rubino M (2008) Processing technologies for poly(lactic acid). Prog Polym Sci 33:820–852. https://doi.org/10.1016/j.progpolymsci.2008.05.004
29. Xinyu W, Qifeng C (2024) Optimization of barrier properties of PLA/PBAT polymers in biodegradable materials. Starch Stärke 2400135:1–14. https://doi.org/10.1002/star.202400135
30. Ma F, Wang B, Leng X et al (2022) Biodegradable PBAT/PLA/CaCO3 blowing films with enhanced mechanical and barrier properties: investigation of size and content of CaCO3 particles. Macromol Mater Eng 307:1–11. https://doi.org/10.1002/mame.202200135
31. Nobrega MM, Bonametti Olivato J, Bona MVEGE, Yamashita F (2010) Effects of the incorporation of saturated fatty acids on the mechanical and barrier properties of biodegradable films. J Appl Polym Sci 116:2658–2667. https://doi.org/10.1002/app
32. Mallegni N, Phuong TV, Coltelli MB et al (2018) Poly(lactic acid) (PLA) based tear resistant and biodegradable flexible films by blown film extrusion. Materials. https://doi.org/10.3390/ma11010148
33. Hassan MM, Koyama K (2020) Thermomechanical and viscoelastic properties of green composites of PLA using chitin microparticles as fillers. J Polym Res. https://doi.org/10.1007/s10965-019-1991-2
34. Olaiya NG, Surya I, Oke PK et al (2019) Properties and characterization of a PLA-chitin-starch biodegradable polymer composite. Polymers. https://doi.org/10.3390/polym11101656
35. Faisant De Champchesnel JB, Tassin JF, Monnerie L et al (1997) Amorphous phase orientation in biaxially drawn poly(ethylene terephthalate) films. Polymer 38:4165–4173. https://doi.org/10.1016/S0032-3861(96)01001-4
36. Wang Y, Zhang H, Li M et al (2015) Orientation and structural development of semicrystalline poly(lactic acid) under uniaxial drawing assessed by infrared spectroscopy and X-ray diffraction. Polym Test 41:163–171. https://doi.org/10.1016/j.polymertesting.2014.11.010
37. Wang Y, Liu L, Li M et al (2015) Spectroscopic analysis of post drawing relaxation in poly(lactic acid) with oriented mesophase. Polym Test 43:103–107. https://doi.org/10.1016/j.polymertesting.2015.03.001
38. Fotie G, Gazzotti S, Ortenzi MA et al (2023) Performance comparison of coatings based on cellulose nanocrystals and microfibrillated cellulose for food packaging. Carbohydrate Polymer Technologies and Applications 5:100264. https://doi.org/10.1016/j.carpta.2022.100264
39. Wang J, Gardner DJ, Stark NM et al (2018) Moisture and oxygen barrier properties of cellulose Nanomaterial-Based films. ACS Sustain Chem Eng 6:49–70. https://doi.org/10.1021/acssuschemeng.7b03523
40. Paulsen E, Lema P, Martínez-Romero D, García-Viguera C (2022) Use of PLA/PBAT stretch-cling film as an ecofriendly alternative for individual wrapping of broccoli heads. Sci Hortic

(Amsterdam) 304:111260. https://doi.org/10.1016/j.scienta.2022.111260
41. Yanat M, Colijn I, Schroën K (2022) Chitin nanocrystals provide antioxidant activity to polylactic acid films. Polymers (Basel). https://doi.org/10.3390/polym14142965
42. Romani VP, Martins VG, Goddard JM (2020) Radical scavenging polyethylene films as antioxidant active packaging materials. Food Control 109:106946. https://doi.org/10.1016/j.foodcont.2019.106946
43. Su LC, Xie Z, Zhang Y et al (2014) Study on the antimicrobial properties of citrate-based biodegradable polymers. Front Bioeng Biotechnol 2:1–9. https://doi.org/10.3389/fbioe.2014.00023
44. Wales A, McLaren I, Rabie A et al (2013) Assessment of the anti-Salmonella activity of commercial formulations of organic acid products. Avian Pathol 42:268–275. https://doi.org/10.1080/03079457.2013.782097
45. Fan J, Zhang J, Yang X et al (2022) Synthesis and properties of sodium fatty acyl lactylates. Colloids Surf Physicochem Eng Asp 653:129946. https://doi.org/10.1016/j.colsurfa.2022.129946
46. Wit JC, De, Rombouts FM (1990) Antimicrobial activity of sodium lactate 6703 HD Wageningen, The Netherlands. Growth (Lakeland)
47. (2011) Commission Regulation (EU) No 10/2011 of 14 January 2011 on plastic materials and articles intended to come into contact with food Text with EEA relevance. 1–89
48. Fortunati E, Puglia D, Kenny JM et al (2013) Effect of ethylene-co-vinyl acetate-glycidylmethacrylate and cellulose microfibers on the thermal, rheological and biodegradation properties of poly(lactic acid) based systems. Polym Degrad Stab 98:2742–2751. https://doi.org/10.1016/j.polymdegradstab.2013.10.007
49. Yang W, Fortunati E, Dominici F et al (2016) Effect of cellulose and lignin on disintegration, antimicrobial and antioxidant properties of PLA active films. Int J Biol Macromol 89:360–368. https://doi.org/10.1016/j.ijbiomac.2016.04.068
50. Mena-Prado I, Reinosa JJ, Fernández-García M et al (2023) Evaluation of poly(lactic acid) and ECOVIO based biocomposites loaded with antimicrobial sodium phosphate microparticles. Int J Biol Macromol. https://doi.org/10.1016/j.ijbiomac.2023.127488
51. Tabasi RY, Ajji A (2015) Selective degradation of biodegradable blends in simulated laboratory composting. Polym Degrad Stab 120:435–442. https://doi.org/https://doi.org/ https://doi.org/10.1016/j.polymdegradstab.2015.07.020
52. Yanat M, Muthurajan M, Strubel M et al (2023) Polylactic acid films reinforced with chitin nanocrystals: biodegradation and migration behavior. Food Packag Shelf Life 40:101217. https://doi.org/10.1016/j.fpsl.2023.101217